Published April 6, 2016, doi:10.4049/jimmunol.1501457

Conditioned Medium from the Stem Cells of Human Exfoliated Deciduous Teeth Ameliorates Experimental Autoimmune Encephalomyelitis

Chiaki Shimojima,* Hideyuki Takeuchi,†,‡ Shijie Jin,† Bijay Parajuli,† Hisashi Hattori,* Akio Suzumura,† Hideharu Hibi,* Minoru Ueda,* and Akihito Yamamoto*

Multiple sclerosis (MS) is a major neuroinflammatory demyelinating disease of the CNS. Current MS treatments, including immunomodulators and immunosuppressants, do not result in complete remission. Stem cells from human exfoliated deciduous teeth (SHEDs) are mesenchymal stem cells derived from dental pulp. Both SHED and SHED-conditioned medium (SHED-CM) exhibit immunomodulatory and regenerative activities and have the potential to treat various diseases. In this study, we investigated the efficacy of SHED-CM in treating experimental autoimmune encephalomyelitis (EAE), a mouse model of MS. EAE mice treated with a single injection of SHED-CM exhibited significantly improved disease scores, reduced demyelination and axonal injury, and reduced inflammatory cell infiltration and proinflammatory cytokine expression in the spinal cord, which was associated with a shift in the microglia/macrophage phenotype from M1 to M2. SHED-CM also inhibited the proliferation of myelin oligodendrocyte glycoprotein–specific CD4$^+$ T cells, as well as their production of proinflammatory cytokines in vitro. Treatment of EAE mice with the secreted ectodomain of sialic acid–binding Ig-like lectin-9, a major component of SHED-CM, recapitulated the effects of SHED-CM treatment. Our data suggest that SHED-CM and secreted ectodomain of sialic acid–binding Ig-like lectin-9 may be novel therapeutic treatments for autoimmune diseases, such as MS. ***The Journal of Immunology*****, 2016, 196: 000–000.**

Multiple sclerosis (MS) and its animal model, experimental autoimmune encephalomyelitis (EAE), are autoimmune neurologic diseases of the CNS (1, 2). MS and EAE are autoreactive Th1 cell– and Th17 cell–mediated diseases, although various types of immune cells and soluble mediators contribute to the complex mechanisms underlying the onset and progression of these diseases. In MS and EAE, autoreactive Th1/Th17 cells infiltrate the CNS, leading to microglia/macrophage activation that induces inflammatory demyelination and subsequent neuronal damage and results in a range of clinical features, including sensory and motor paralysis, blindness, pain, incontinence, and dementia.

Previous studies showed that the transplantation of various types of stem cells and their derivatives, including human bone marrow mesenchymal stem cells (BMMSCs) (3, 4) adipogenic stem cells (5), placenta-derived stem cells (6), and neural precursor cells (7), promotes functional recovery in animal models of MS. However, the results of most studies indicate that the engrafted cells undergo minimal differentiation in vivo and survive for only short periods of time. In addition, recent studies showed that mesenchymal stem cells (MSCs) infused peripherally are prevented from infiltrating into the CNS and instead act peripherally to inhibit CNS inflammation. Several lines of evidence suggest that transplanted MSCs can protect neural tissue through cell replacement and/or paracrine mechanisms (8–10); however, it is unclear whether the paracrine factors alone, without the cell graft, would show therapeutic benefit in the treatment of EAE.

Stem cells from human exfoliated deciduous teeth (SHEDs) are derived from normal dental pulp. They are thought to originate from the cranial neural crest and express early mesenchymal and neuroectodermal stem cell markers (11). In addition, they can differentiate into functional neurons and oligodendrocytes under the appropriate conditions (12–14). SHEDs exhibit immunomodulatory and regenerative activities and have the potential to treat various diseases. We showed previously that SHED transplantation into completely transected rat spinal cord resulted in the functional recovery of hind limb locomotion (14). Moreover, SHED engraftment promotes functional recovery from various acute and chronic CNS insults through paracrine mechanisms that activate endogenous tissue-repairing activity (15, 16). Furthermore, these studies showed that SHED-conditioned medium (SHED-CM) exerts similar therapeutic effects to those of SHEDs, including remyelination of the CNS. The major drivers of this

*Department of Oral and Maxillofacial Surgery, Nagoya University Graduate School of Medicine, Showa-ku, Nagoya 466-8550, Japan; †Department of Neuroimmunology, Research Institute of Environmental Medicine, Nagoya University, Chikusa-ku, Nagoya 464-8601, Japan; and ‡Department of Neurology and Stroke Medicine, Yokohama City University Graduate School of Medicine, Kanazawa-ku, Yokohama 236-0004, Japan

ORCIDs: 0000-0001-5912-7581 (H.T.); 0000-0003-3813-113X (B.P.); 0000-0001-9181-8948 (H. Hattori); 0000-0003-0248-7476 (H. Hibi); 0000-0002-9206-1243 (A.Y.).

Received for publication June 29, 2015. Accepted for publication March 14, 2016.

Address correspondence and reprint requests to Dr. Akihito Yamamoto or Dr. Hideyuki Takeuchi, Department of Oral and Maxillofacial Surgery, Nagoya University Graduate School of Medicine, 65 Tsurumai-cho, Showa-ku, Nagoya 466-8550, Japan (A.Y.) or Department of Neurology and Stroke Medicine, Yokohama City University Graduate School of Medicine, 3-9 Fukuura, Kanazawa-ku, Yokohama 236-0004, Japan (H.T.). E-mail addresses: akihito@med.nagoya-u.ac.jp. (A.Y.) or htake@yokohama-cu.ac.jp (H.T.)

The online version of this article contains supplemental material.

Abbreviations used in this article: BMMSC, bone marrow mesenchymal stem cell; BMMSC-CM, CM from BMMSC; CM, conditioned medium; EAE, experimental autoimmune encephalomyelitis; ED–Siglec-9, ectodomain of sialic acid–binding Ig-like lectin-9; HGF, hepatocyte growth factor; iNOS, inducible NO synthase; LFB, Luxol fast blue; MBP, myelin basic protein; MOG, myelin oligodendrocyte glycoprotein; $MOG_{35–55}$, MOG peptide 35–55; $^{MOG}CD4^+$ T cell, $MOG_{35–55}$-specific CD4$^+$ T cell; MS, multiple sclerosis; MSC, mesenchymal stem cell; qPCR, quantitative PCR; SHED, stem cell from human exfoliated deciduous teeth; SHED-CM, SHED-conditioned medium.

regenerative process are peripherally derived macrophages involved in resolving inflammation.

Macrophages are composed of distinct subpopulations, including the classically activated M1 and alternatively activated M2 polarized macrophages. M1 macrophages initiate inflammation by releasing high levels of proinflammatory cytokines, glutamate, reactive oxygen, and NO and are implicated in CNS autoimmune disease via their secretion of toxic molecules and Ag presentation to cytotoxic lymphocytes. In contrast, M2 macrophages counteract proinflammatory conditions and promote tissue repair by secreting anti-inflammatory cytokines (17). They also promote remyelination through the phagocytosis of myelin debris and secretion of cytokines (18).

We showed previously that SHED-CM improved a rodent model of spinal cord injury, liver inflammation, lung fibrosis, rheumatoid arthritis, and Alzheimer's disease by inducing macrophage phenotype conversion from M1 to M2 (19–23). SHED-CM contains a set of M2-inducing molecules, including MCP-1 and the secreted ectodomain of sialic acid-binding Ig-like lectin-9 (ED–Siglec-9), which promote functional recovery from spinal cord injury (23). In addition, we showed that ED–Siglec-9 was uniquely expressed in SHED-CM compared with the CM from BMMSCs (BMMSC-CM) and from fibroblasts (23).

In this study, we examined the therapeutic benefits of SHED-CM and ED–Siglec-9 in treating EAE. A single injection of SHED-CM or ED–Siglec-9 markedly improved EAE, whereas the depletion of ED–Siglec-9 from SHED-CM abrogated these effects. Our findings suggest that SHED-CM and ED–Siglec-9 may provide significant therapeutic benefits for treating autoimmune diseases, such as MS.

Materials and Methods

EAE mice

The protocols for animal experiments were approved by the Animal Experiment Committee and Research Ethics Committee of Nagoya University (approval number 14018). C57BL/6J mice were purchased from Japan SLC (Hamamatsu, Japan). EAE was induced as described previously (24, 25). Briefly, 8-wk-old female C57BL/6J mice were immunized s.c. at the base of the tail with 0.2 ml an emulsion containing 200 μg myelin oligodendrocyte glycoprotein (MOG) peptide 35–55 ($MOG_{35–55}$; MEVGWYRSPFSRVVHLYRNGK; Operon Biotechnologies, Tokyo, Japan) in saline combined with an equal volume of CFA (Sigma-Aldrich, St. Louis, MO) containing 300 ml heat-killed *Mycobacterium tuberculosis* H37Ra (Difco, Detroit, MI). The mice were injected i.p. with 200 ng pertussis toxin (List Biological Laboratories, Campbell, CA) on days 0 and 2 postimmunization. The mice were assessed daily for clinical signs of EAE, according to the following grading system: 0, normal; 1, limp tail or mild hind limb weakness; 2, moderate hind limb weakness or mild ataxia; 3, moderate to severe hind limb weakness; 4, severe hind limb weakness, mild fore limb weakness, or moderate ataxia; 5, paraplegia with moderate fore limb weakness; and 6, paraplegia with severe fore limb weakness, severe ataxia, or moribundity.

Preparation of SHED-CM and treatment protocols

SHED and SHED-CM were prepared as described previously (14, 23). In brief, exfoliated deciduous teeth (from 6- to 12-y-old children), which were extracted for clinical purposes, were collected at Nagoya University School of Medicine under the approved guidelines set by Nagoya University (H-73, 2003). Ethical approval was obtained from the ethics committee of Nagoya University (permission number 8-2). All participants provided written informed consent. After separating the crown and root, the dental pulp was isolated and digested in a solution of 3 mg/ml Collagenase type I and 4 mg/ml Dispase for 1 h at 37°C. Single-cell suspensions ($1–2 \times 10^4$ cells/ml) were plated on culture dishes in DMEM supplemented with 10% FCS (both from Sigma-Aldrich) and incubated at 37°C in an atmosphere containing 5% CO_2 at 100% humidity. The SHEDs used in this study exhibited a fibroblastic morphology with a bipolar spindle shape, expressed MSC markers (CD90, CD73, and CD105) but not endothelial/hematopoietic markers (CD34, CD45, CD11b/c, or HLA-DR), and exhibited adipogenic, chondrogenic, and osteogenic differentiation. The majority of SHEDs coexpressed several neural lineage markers: nestin, doublecortin, βIII-tubulin, NeuN, GFAP, S-100, A2B5, and CNPase. They can differentiate into functional neurons and oligodendrocytes under the appropriate conditions.

After three to nine passages, SHEDs at 70–80% confluency were washed with PBS twice, and the culture medium was replaced with serum-free DMEM. After a 48-h incubation, the medium was collected and centrifuged for 3 min at 440 × *g*. The supernatants were collected and centrifuged for 3 min at 4°C and 17,400 × *g*. The resulting supernatants were used as SHED-CM in various experiments. The protein concentration in SHED-CM was measured using a BCA Protein Assay Kit (Pierce, Rockford, IL) and adjusted to 3 μg/ml with DMEM. SHED-CM or control DMEM (500 μl) was injected i.v. at day 14 postimmunization, at the peak of EAE.

CM cytokine measurement and protein-depletion assay

The levels of ED–Siglec-9 and hepatocyte growth factor (HGF) in CM samples were determined by ELISA (RayBio Human Siglec-9 ELISA Kit; Ray Biotech, Norcross, GA; Human HGF ELISA Kit, R&D Systems, Minneapolis, MN). To deplete the SHED-CM of ED–Siglec-9 or HGF, anti–Siglec-9 or anti-HGF Abs, prebound to Protein G–Sepharose (GE Healthcare, Piscataway, NJ), were added to SHED-CM. The mixtures were incubated overnight at 4°C, and the Ab beads were removed by centrifugation. The depletion of ED–Siglec-9 and HGF was confirmed by ELISA.

Histological analysis

EAE mice were anesthetized and perfused intracardially with PBS on day 28 postimmunization. The lumbosacral spinal cords were fixed with 4% paraformaldehyde and embedded in paraffin or OCT compound (Sakura Finetek Japan, Tokyo, Japan). The frozen sections (8 μm) were stained with H&E, Luxol fast blue (LFB), and Sudan black B. The paraffin sections (4 μm) were subjected to anti-myelin basic protein (MBP) immunostaining. Briefly, deparaffinized and rehydrated sections were blocked with 5% bovine serum for 30 min after Ag retrieval and incubated overnight with mouse anti-MBP mAb (1:1000; Merck Millipore, Billerica, MA). Then, diaminobenzidine was used to develop a subsequent polymer reagent (ENVISION kit/HRP [DAB]; DAKO, Glostrup, Denmark). The sections were counterstained with hematoxylin. The lumbosacral spinal cords were also postfixed in 1% osmium tetroxide, dehydrated, and embedded in epoxy resin. One-micron sections were stained with Toluidine Blue. The demyelinated lesions were identified as the unstained areas in the LFB, Sudan black B, anti-MBP, and Toluidine Blue–stained sections.

For immunofluorescence staining, the frozen sections (20 μm) were permeabilized with 0.1% Triton X-100 in PBS for 20 min, blocked with 5% bovine serum for 30 min, and incubated overnight with rabbit anti-mouse CD3 polyclonal Abs (1:100; Abcam, Cambridge, U.K.), mouse anti-phosphorylated neurofilament mAb (SMI31, 1:500; Sternberger Monoclonals, Lutherville, MD), rat anti-mouse F4/80 mAb (CI:A3-1, 1:1000; AbD Serotec, Raleigh, NC), rabbit anti-mouse inducible NO synthase (iNOS) polyclonal Abs (1:5000; Merck Millipore), and goat anti-mouse Arginase-1 polyclonal Abs (1:200; Proteintech), followed by incubation with Alexa Fluor 488, Alexa Fluor 546, or Alexa Fluor 647–conjugated secondary Abs (Life Technologies, Carlsbad, CA). The stained cells were analyzed in six random fields/section using a deconvolution fluorescence microscope system (BZ-8000; Keyence, Osaka, Japan). Data were collected from three animals/group.

RNA extraction and RT-PCR

Total RNA was isolated from the lumbar spinal cord of EAE mice on day 16 postimmunization using an RNeasy Mini Kit (QIAGEN, Valencia, CA) and reverse transcribed with SuperScript III (Invitrogen, Carlsbad, CA). The levels of mRNAs encoding TNF-α, IL-17, IFN-γ, iNOS, and Arginase-1 were evaluated by quantitative PCR (qPCR) using THUNDERBIRD SYBR qPCR Mix (Toyobo, Osaka, Japan) on the StepOnePlus Real-Time PCR System (Applied Biosystems, Foster City, CA). Gene expression values were determined using the $\Delta\Delta C_T$ method. The genes of interest were standardized to the geometric mean of GAPDH. Three independent assays were performed. The mouse primers used are shown in Supplemental Table I.

MOG-specific $CD4^+$ T cell culture

MOG-specific $CD4^+$ T cells were isolated from the spleen of EAE mice on day 14 postimmunization using the MACS system (Miltenyi Biotec, Bergisch Gladbach, Germany). The isolated $CD4^+$ T cells (2×10^5

cells/well) were cultured with mitomycin C–treated feeder cells (5×10^5 cells/well) in SHED-CM or DMEM in the presence of $MOG_{35–55}$ (20 ng/ml) for 72 h. The supernatants were collected for cytokine analysis, and the cells were analyzed using a BrdU cell proliferation assay (Calbiochem, San Diego, CA). The concentrations of IL-17, IFN-γ, and IL-2 were assessed using the corresponding cytokine-specific ELISA kits (IL-17, IFN-γ, R&D Systems; IL-2, BD Biosciences, Franklin Lakes, NJ), as described previously (24, 25). Six independent assays were performed.

Bone marrow–derived macrophage culture

Bone marrow cells were isolated from adult female C57BL/6J mice as described previously (23). They were plated at 3×10^6 cells/24-well plate and differentiated into macrophages in DMEM supplemented with 20 ng/ml M-CSF (PeproTech) for 7 d. The macrophages were assessed 24 h after incubation with serum-free DMEM, SHED-CM, 100 ng/ml ED–Siglec-9, or 100 ng/ml ED–Siglec-9/MCP-1.

Effector $CD4^+$ T cell differentiation

$CD4^+CD62L^+$ T cells were isolated from the spleen and lymph nodes of 8-wk-old female C57BL/6J mice using MACS beads (Miltenyi Biotec), as described previously (26). Cells (2×10^5 cells/well) were stimulated with plate-bound anti-CD3 Abs (5 mg/ml; 145-2C11) and soluble anti-CD28 Abs (2 mg/ml; 37.51; both from BD Biosciences) for 6 d in RPMI 1640 medium supplemented with 2 mM sodium pyruvate, L-glutamine, 10% FBS, and IL-2 (20 ng/ml) in the presence of 50% DMEM, 50% SHED-CM, or 100 ng/ml ED–Siglec-9/MCP-1. T cells were polarized with recombinant mouse IL-12 (10 ng/ml; R&D Systems), mouse IFN-γ (5 ng/ml; R&D Systems) plus anti–IL-4 (11B.11, 10 mg/ml; BD Biosciences) for Th1, mouse IL-4 (2 ng/ml; R&D Systems) plus anti–IFN-γ (XMG1.2, 10 mg/ml; BD Biosciences) for Th2, human TGF-β1 (5 ng/ml), IL-6 (30 ng/ml) plus anti–IFN-γ for Th17. The concentrations of IFN-γ, IL-4, and IL-17 in the culture supernatant were measured by each specific ELISA (IFN-γ and IL-4, BD Biosciences; IL-17, R&D Systems).

Statistical analysis

Statistical significance was analyzed with the Student *t* test or one-way ANOVA, followed by the post hoc Tukey test, using SPSS 19.0.

Results

A single injection of SHED-CM ameliorates the clinical severity of EAE

First, we evaluated the therapeutic effects of SHED-CM on $MOG_{35–55}$-induced EAE. Mice were injected i.v. with SHED-CM or DMEM at the peak of EAE (day 14 postimmunization, average clinical score 3–4). As shown in Fig. 1, mice receiving only a single administration of SHED-CM exhibited significantly reduced disease severity compared with those treated with DMEM. These data suggested that a single injection of SHED-CM during the chronic phase of EAE can result in rapid and sustained improvements in its pathology.

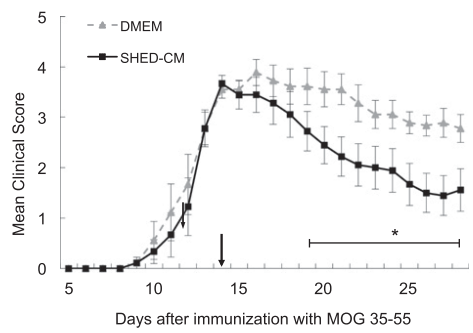

FIGURE 1. A single administration of SHED-CM ameliorates EAE severity. Treatment with SHED-CM (500 μl), but not DMEM (500 μl), at the peak of EAE (day 14 postimmunization with $MOG_{35–55}$ peptide, arrow) ameliorated the severity of EAE. Data are mean ± SEM (n = 9/group). *$p < 0.05$.

Treatment with SHED-CM reduces inflammatory cell infiltration, demyelination, and axonal injury in the EAE spinal cord

EAE severity depends on the extent of demyelination and inflammatory cell infiltration in the CNS. Histological examination of tissue sections was performed 2 wk after a single injection of SHED-CM or DMEM, on day 28 postimmunization. LFB, Sudan black B, anti-MBP, and Toluidine Blue staining were used to detect demyelination, and H&E anti-CD3 staining was used to evaluate inflammatory cell infiltration. Compared with sections from the DMEM-treated group, which showed substantial demyelination and immune cell infiltration, sections from the SHED-CM–treated group exhibited reduced demyelination, with most of the white matter having a normal appearance (Fig. 2A, 2B), as well as a reduction in inflammatory cell infiltration (Fig. 2A, 2C). Furthermore, we evaluated axonal injury by SMI31 immunostaining. Previously, we reported that bead-like swelling along axons (axonal beading) is a good pathological marker of axonal injury resulting from axonal transport impairment (27–29). The reduction in axonal beading is associated with recovery from EAE (30). In this study, DMEM-treated mice also showed axonal loss and axonal beading (cross section area = 40–80 μm^2) in the demyelinated lesions, and SHED-CM treatment significantly improved this axonal injury (Fig. 2D, 2E). These results indicated that functional improvements mediated by a single injection of SHED-CM were associated with reduced demyelination, inflammatory cell infiltration, and axonal injury in the CNS.

SHED-CM suppresses proinflammatory cytokine expression in the EAE spinal cord

To investigate the anti-inflammatory effects of SHED-CM, the lumbar spinal cords were collected from EAE mice treated with DMEM or SHED-CM 48 h after treatment. qPCR analyses revealed that the expression levels of the proinflammatory cytokines IFN-γ, IL-17, and TNF-α were suppressed in the SHED-CM–treated mice compared with the DMEM-treated ones (Fig. 3A). In addition, SHED-CM treatment upregulated the expression of the mRNAs encoding the M2 markers Arginase-1 and CD206 and downregulated the expression of the mRNA encoding the M1 marker iNOS (Fig. 3A).

Immunostaining data corroborated these results as a decrease in the $F4/80^+iNOS^+$ M1 subpopulation and an increase in the $F4/80^+$ $Arginase\text{-}1^+$ M2 subpopulation in SHED-CM–treated mice compared with DMEM-treated mice (Fig. 3B). These data indicated that SHED-CM induced an M1 to M2 macrophage conversion, leading to the suppression of proinflammatory mediators.

SHED-CM inhibits $MOG_{35–55}$-specific $CD4^+$ T cell proliferation and production of proinflammatory cytokines

Because $MOG_{35–55}$-specific $CD4^+$ T cells ($^{MOG}CD4^+$ T cells) play an important role in EAE disease progression, we next examined the effect of SHED-CM on the activation of these cells. Splenic $^{MOG}CD4^+$ T cells isolated from mice at the peak of EAE were stimulated with $MOG_{35–55}$ peptide and cultured in SHED-CM or DMEM with feeder cells for 3 d. Analysis of the cells with a BrdU-incorporation assay and IL-2 ELISA showed that SHED-CM significantly suppressed the $^{MOG}CD4^+$ T cell proliferation in vitro (Fig. 4A). The production of IFN-γ and IL-17 was also suppressed in the SHED-CM–treated group compared with the DMEM-treated group (Fig. 4B). These results demonstrated that SHED-CM affected the recall response of $^{MOG}CD4^+$ T cells and inhibited their proliferation and subsequent production of Th1/Th17 proinflammatory cytokines.

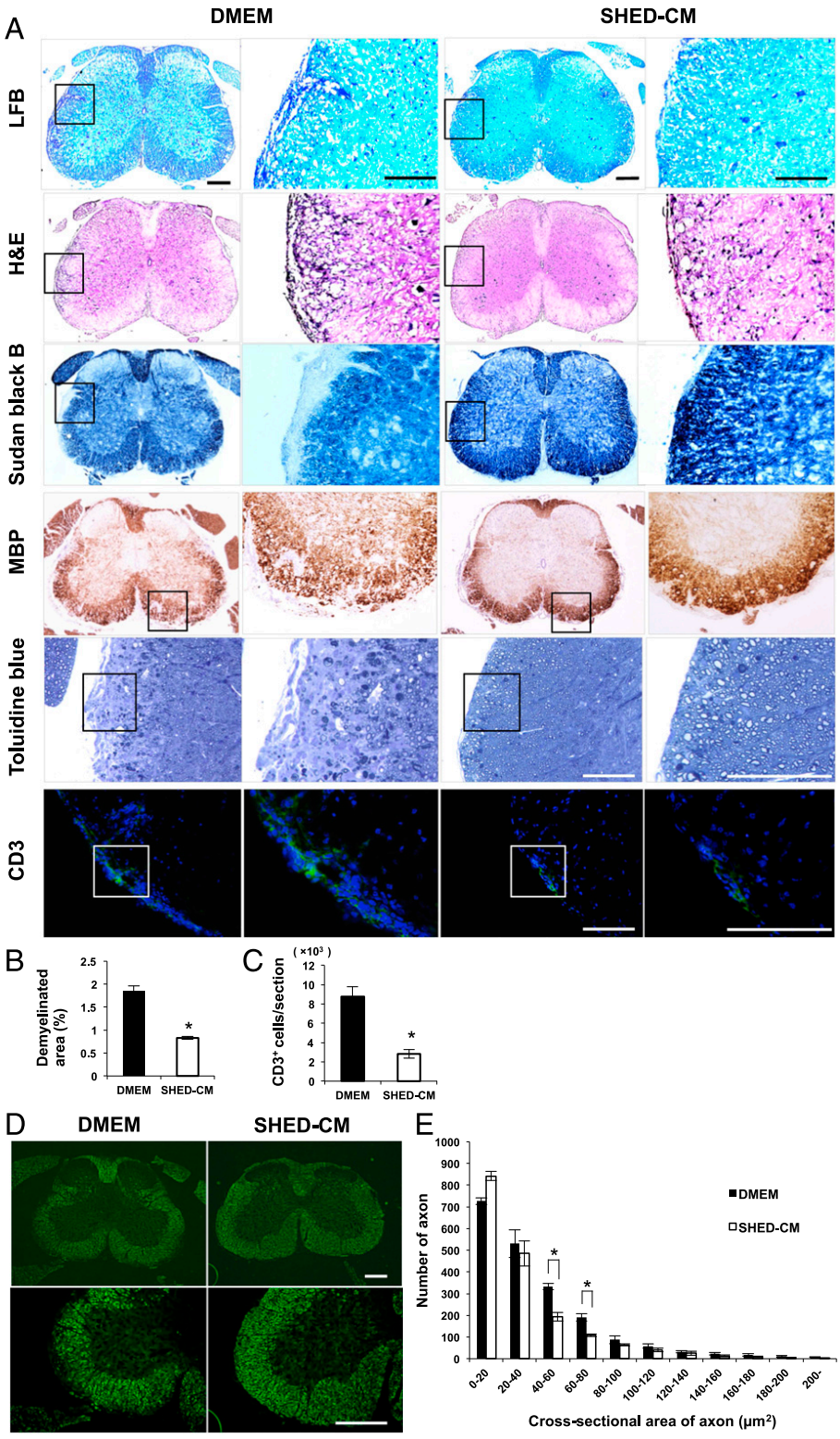

FIGURE 2. SHED-CM reduces inflammation, demyelination, and axonal injury in the EAE spinal cord. Spinal cord sections were prepared on day 28 postimmunization. (**A**) LFB, Sudan black B, anti-MBP, and Toluidine Blue staining were used to detect the demyelinated areas. H&E and anti-CD3 staining were used to monitor inflammatory cell infiltration. Quantification of the demyelinated areas (**B** and **C**) and $CD3^+$ cells (**D**) in the sections. (D) Axon staining with SMI31 was used to indicate the axonal injury. (**E**) Quantification of each cross-sectional area of axons. SHED-CM treatment significantly suppressed bead-like axonal injury (axonal beading, 40–80 μm^2). Data are mean ± SEM ($n = 3$). Scale bars, 250 μm. *$p < 0.05$.

HGF depletion has little effect on the in vivo efficacy of SHED-CM

SHED-CM contains a variety of growth factors, including HGF (23). HGF is reported to promote angiogenesis and tissue regeneration and to suppress chronic inflammation in various disease models (31–33). Therefore, to determine whether the in vivo efficacy of SHED-CM is dependent on HGF, we treated EAE mice with HGF-depleted SHED-CM. The depletion of HGF from SHED-CM was confirmed using an HGF ELISA (Supplemental Table II). Unexpectedly, mice treated with a single injection of HGF-depleted SHED-CM showed significant improvements in EAE (Fig. 5). These data showed that HGF had little effect on the in vivo efficacy of SHED-CM.

ED–Siglec-9 recapitulates the in vivo efficacy of SHED-CM

ED–Siglec-9 is also a major component of SHED-CM, although it is barely detectable in BMMSC-CM or in the CM from fibroblasts. Moreover, we recently reported that ED–Siglec-9 and MCP-1 synergistically promote recovery in a rat model of spinal cord injury by altering the macrophage polarity toward the anti-inflammatory M2

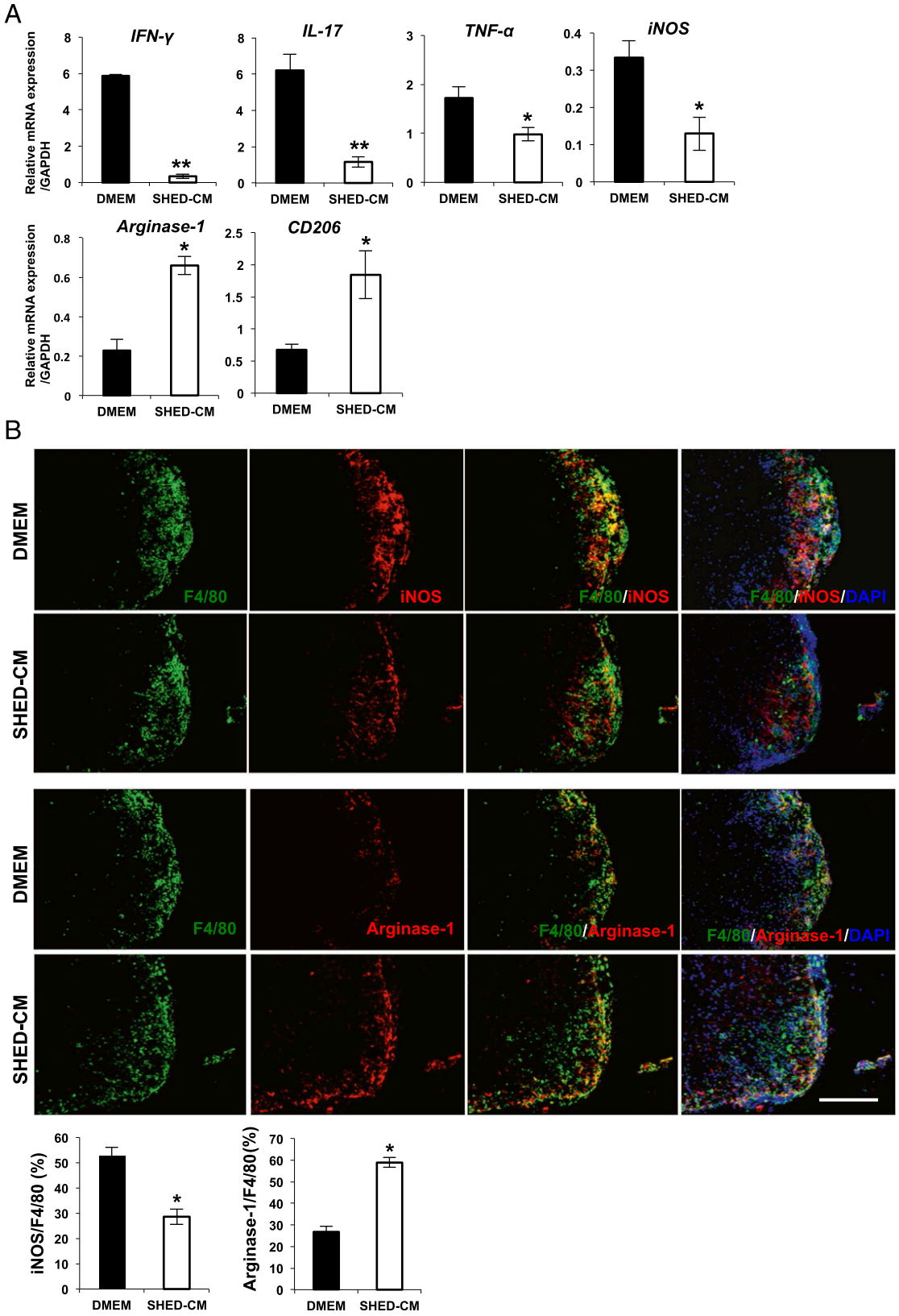

FIGURE 3. Treatment with SHED-CM suppresses the expression of proinflammatory cytokines in the EAE spinal cord. qPCR analysis of the spinal cords from SHED-CM–treated and DMEM-treated groups. (**A**) SHED-CM significantly suppressed the expression of mRNAs encoding proinflammatory cytokines, such as IFN-γ, IL-17, and TNF-α, and downregulated M1 markers and upregulated M2 markers. (**B**) Representative immunohistological images of EAE spinal cord sections 48 h after SHED-CM or DMEM administration. Proinflammatory M1 macrophages (iNOS) and anti-inflammatory M2 macrophages (Arginase-1) were examined. The number of Arginase-1$^+$ F4/80$^+$ M2 cells was increased in SHED-CM–treated spinal cord, whereas the number of iNOS$^+$ F4/80$^+$ M1 cells was decreased. Scale bars, 250 μm. Data are mean ± SEM ($n = 4$). *$p < 0.05$, **$p < 0.01$.

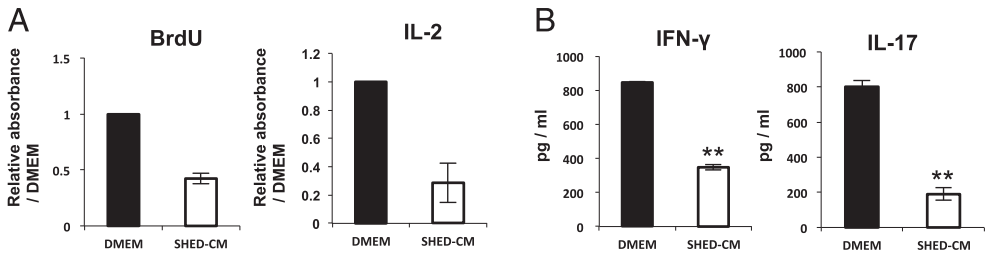

FIGURE 4. SHED-CM inhibits the proliferation of MOG-specific $CD4^+$ T cells and reduces their production of proinflammatory cytokines. (**A**) MOG-specific $CD4^+$ T cell proliferation and IL-2 production in vitro were analyzed by BrdU incorporation and an IL-2 ELISA. (**B**) The production levels of IFN-γ and IL-17 in the SHED-CM and DMEM treatment groups were evaluated by ELISA. Data are mean ± SEM ($n = 4$). $^{**}p < 0.01$.

state (23). Previous studies showed that the level of endogenous MCP-1 is upregulated at the peak of EAE (34, 35). Therefore, to examine whether treatment with ED–Siglec-9 alone would improve the symptoms of EAE, mice at the peak of disease were treated with a single injection of recombinant ED–Siglec-9, ED-Siglec-9–depleted SHED-CM, or DMEM. We confirmed the depletion of ED–Siglec-9 and the presence of HGF by ELISA (Supplemental Table II). Notably, mice treated with recombinant ED–Siglec-9 showed significant improvement, whereas mice treated with ED–Siglec-9–depleted SHED-CM or DMEM exhibited severe EAE, with clinical scores of 3 to 4 (Fig. 6). These data indicated that ED–Siglec-9 was the critical factor responsible for the efficacy of SHED-CM in treating EAE.

MCP-1 and ED–Siglec-9 synergistically induce M2 macrophages but have little effect on T cell differentiation

We reported that MCP-1 and ED–Siglec-9 synergistically induce M2 differentiation of rat bone marrow–derived macrophages, whereas either of them alone has little effect (23). M1 and M2 macrophages are known to exhibit distinct shapes (i.e., M1 macrophages are round; M2 macrophages are elongated) (36). Our results showed that mouse bone marrow–derived macrophages treated with DMEM or ED–Siglec-9 were spherical, whereas those treated with SHED-CM or ED–Siglec-9/MCP-1 were elongated and expressed a high level of CD206 (Supplemental Fig. 1).

Next, we investigated whether ED–Siglec-9 affects effector $CD4^+$ T cell differentiation. T cells were polarized with IL-12, IFN-γ plus anti–IL-4 for Th1, IL-4 plus anti–IFN-γ for Th2, and TGF-β1, IL-6, and anti–IFN-γ for Th17 (*Materials and Methods*). We found that SHED-CM and ED–Siglec-9/MCP-1 had little effect on Th1/Th2/Th17 cell differentiation (data not shown). Taken together, these findings suggest that SHED-CM and ED–Siglec-9/MCP-1 directly modulate the polarity of macrophages but not naive T cells.

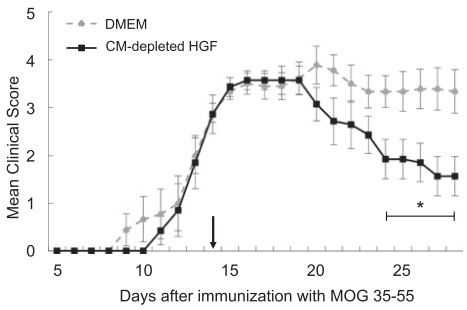

FIGURE 5. Depletion of HGF does not affect the in vivo efficacy of SHED-CM. Treatment of mice with HGF-depleted SHED-CM (500 μl) at the peak of EAE (day 14 postimmunization, arrow) significantly suppressed the severity of EAE. Data are mean ± SEM ($n = 8$/group). $^{*}p < 0.05$.

Discussion

We showed that treating mice with a single i.v. injection of human SHED-CM reduced the severity of EAE by suppressing the neuroinflammation, demyelination, and axonal injury associated with this disease. Analysis of the spinal cord of treated mice showed that SHED-CM induced a shift in the macrophage phenotype from an M1 proinflammatory phenotype to an M2 anti-inflammatory phenotype, as well as suppressed the expression of proinflammatory mediators. Treatments resulting in shifts from M1 to M2 phenotypes were shown to suppress EAE (37, 38). In addition, our in vitro analysis indicated that the presence of SHED-CM inhibited the proliferation of $^{MOG}CD4^+$ T cells and suppressed their production of proinflammatory Th1/Th17 cytokines. Thus, our data suggested that SHED-CM can suppress the proliferation of autoreactive Th1/Th17 cells, although it is unclear whether this effect is direct or indirect in vivo. Taken together, these findings indicated that the SHED-CM–induced modulation of the microenvironment resulted in suppressed demyelination and improved EAE symptoms.

SHED-CM contains a variety of growth factors, including neurotrophic factors, which promote such effects as neuroprotection, axonal elongation, neurotransmission, and immunosuppression. Previous reports showed that several factors, including indoleamine 2,3-dioxygenase, IL-6, PGE_2, LIF, and HGF, contribute to the immunosuppressive effects of MSCs (39–43). HGF, in particular, is thought to be the critical factor in human BMMSCs that promotes tissue regeneration and drives the antiproliferative effect on T cells (42). HGF is also one of the most abundant components of SHED-CM, by cytokine Ab array analysis; however, our previous study identified ED–Siglec-9 as another major component of SHED-CM. Furthermore, we showed that ED–Siglec-9 and MCP-1 in SHED-CM could synergistically alter the M1/M2 polarity of macrophages/microglia in vivo (23).

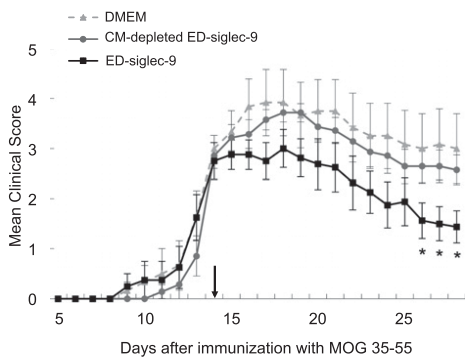

FIGURE 6. ED–Siglec-9 recapitulates the in vivo efficacy of SHED-CM. Treatment of mice with ED–Siglec-9 (500 ng) at the peak of EAE (day 14 postimmunization, arrow) significantly suppressed EAE, whereas treatment with ED-Siglec-9–depleted SHED-CM (500 μl) or DMEM (500 μl) showed no significant improvement. Data are mean ± SEM ($n = 8$/group). $^{*}p < 0.05$.

Although the effect of SHED-CM on EAE depends on ED–Siglec-9, SHED-CM–treated mice showed somewhat better recovery than ED-Siglec-9–treated ones, suggesting that the other factor(s) in SHED-CM, including HGF, might cooperatively improve EAE.

Because MCP-1 is known to be upregulated in EAE (34, 35), we focused our efforts on investigating the therapeutic potential of ED–Siglec-9. Although sialic acid–binding Ig-like lectin-9 is a type I transmembrane protein that functions as a receptor, its secreted ectodomain functions as a ligand. Notably, the full-length transmembrane form of sialic acid–binding Ig-like lectin-9 is found at similar levels in BMMSC, fibroblast, and SHED cell lysates, whereas secreted ED–Siglec-9 is expressed uniquely in SHED-CM (23). In this study, we demonstrated that a single dose of ED–Siglec-9 recapitulated the therapeutic effects of SHED-CM on EAE. It is possible that ED–Siglec-9 functions by interacting with the sialic acid–bound CCR2 to induce M2 macrophage polarization, as shown previously (23). However, future studies will be required to determine the specific mechanism underlying the ED-Siglec-9–mediated improvement in EAE.

Taken together, our studies suggest that SHED-CM and ED–Siglec-9 have the potential to provide multiple benefits in treating autoimmune disease. The finding that a single i.v. injection of CM or recombinant ED–Siglec-9, administered at the peak of EAE, resulted in sustained disease improvement suggests that they may be highly efficacious treatments with long-term effects. SHED-CM was shown to have unique immunomodulatory abilities in the EAE mouse; it suppressed inflammation and induced an anti-inflammatory microenvironment. Furthermore, SHED-CM showed therapeutic efficacy in other models of inflammation, including the rat spinal cord injury model and hypoxic-ischemic brain injury in neonatal mice (14, 16). In addition, SHED-CM and ED–Siglec-9 may represent safer cell-free options compared with MSC treatments that have been used clinically for a decade, although their long-term tumorigenic risk is still unknown.

In summary, we showed that a single injection of SHED-CM or ED–Siglec-9 significantly improved EAE. The results of these and further studies may provide new cell-free therapies for autoimmune diseases, such as MS.

Disclosures

The authors have no financial conflicts of interest.

References

1. Hemmer, B., J. J. Archelos, and H. P. Hartung. 2002. New concepts in the immunopathogenesis of multiple sclerosis. *Nat. Rev. Neurosci.* 3: 291–301.
2. Takeuchi, H. 2014. Midkine and multiple sclerosis. *Br. J. Pharmacol.* 171: 931–935.
3. Bai, L., D. P. Lennon, V. Eaton, K. Maier, A. I. Caplan, S. D. Miller, and R. H. Miller. 2009. Human bone marrow-derived mesenchymal stem cells induce Th2-polarized immune response and promote endogenous repair in animal models of multiple sclerosis. *Glia* 57: 1192–1203.
4. Gordon, D., G. Pavlovska, J. B. Uney, D. C. Wraith, and N. J. Scolding. 2010. Human mesenchymal stem cells infiltrate the spinal cord, reduce demyelination, and localize to white matter lesions in experimental autoimmune encephalomyelitis. *J. Neuropathol. Exp. Neurol.* 69: 1087–1095.
5. Yousefi, F., M. Ebtekar, M. Soleimani, S. Soudi, and S. M. Hashemi. 2013. Comparison of in vivo immunomodulatory effects of intravenous and intraperitoneal administration of adipose-tissue mesenchymal stem cells in experimental autoimmune encephalomyelitis (EAE). *Int. Immunopharmacol.* 17: 608–616.
6. Fisher-Shoval, Y., Y. Barhum, O. Sadan, S. Yust-Katz, T. Ben-Zur, N. Lev, C. Benkler, M. Hod, E. Melamed, and D. Offen. 2012. Transplantation of placenta-derived mesenchymal stem cells in the EAE mouse model of MS. *J. Mol. Neurosci.* 48: 176–184.
7. Chen, L., R. Coleman, R. Leang, H. Tran, A. Kopf, C. M. Walsh, I. Sears-Kraxberger, O. Steward, W. B. Macklin, J. F. Loring, and T. E. Lane. 2014. Human neural precursor cells promote neurologic recovery in a viral model of multiple sclerosis. *Stem Cell Rep.* 2: 825–837.
8. Uccelli, A., L. Moretta, and V. Pistoia. 2008. Mesenchymal stem cells in health and disease. *Nat. Rev. Immunol.* 8: 726–736.
9. Uccelli, A., and D. J. Prockop. 2010. Why should mesenchymal stem cells (MSCs) cure autoimmune diseases? *Curr. Opin. Immunol.* 22: 768–774.
10. Drago, D., C. Cossetti, N. Iraci, E. Gaude, G. Musco, A. Bachi, and S. Pluchino. 2013. The stem cell secretome and its role in brain repair. *Biochimie* 95: 2271–2285.
11. Miura, M., S. Gronthos, M. Zhao, B. Lu, L. W. Fisher, P. G. Robey, and S. Shi. 2003. SHED: stem cells from human exfoliated deciduous teeth. *Proc. Natl. Acad. Sci. USA* 100: 5807–5812.
12. Arthur, A., G. Rychkov, S. Shi, S. A. Koblar, and S. Gronthos. 2008. Adult human dental pulp stem cells differentiate toward functionally active neurons under appropriate environmental cues. *Stem Cells* 26: 1787–1795.
13. Király, M., B. Porcsalmy, A. Pataki, K. Kádár, M. Jelitai, B. Molnár, P. Hermann, I. Gera, W. D. Grimm, B. Ganss, et al. 2009. Simultaneous PKC and cAMP activation induces differentiation of human dental pulp stem cells into functionally active neurons. *Neurochem. Int.* 55: 323–332.
14. Sakai, K., A. Yamamoto, K. Matsubara, S. Nakamura, M. Naruse, M. Yamagata, K. Sakamoto, R. Tauchi, N. Wakao, S. Imagama, et al. 2012. Human dental pulp-derived stem cells promote locomotor recovery after complete transection of the rat spinal cord by multiple neuro-regenerative mechanisms. *J. Clin. Invest.* 122: 80–90.
15. Inoue, T., M. Sugiyama, H. Hattori, H. Wakita, T. Wakabayashi, and M. Ueda. 2013. Stem cells from human exfoliated deciduous tooth-derived conditioned medium enhance recovery of focal cerebral ischemia in rats. *Tissue Eng. Part A* 19: 24–29.
16. Yamagata, M., A. Yamamoto, E. Kako, N. Kaneko, K. Matsubara, K. Sakai, K. Sawamoto, and M. Ueda. 2013. Human dental pulp-derived stem cells protect against hypoxic-ischemic brain injury in neonatal mice. *Stroke* 44: 551–554.
17. Edwards, J. P., X. Zhang, K. A. Frauwirth, and D. M. Mosser. 2006. Biochemical and functional characterization of three activated macrophage populations. *J. Leukoc. Biol.* 80: 1298–1307.
18. Kotter, M. R., C. Zhao, N. van Rooijen, and R. J. M. Franklin. 2005. Macrophage-depletion induced impairment of experimental CNS remyelination is associated with a reduced oligodendrocyte progenitor cell response and altered growth factor expression. *Neurobiol. Dis.* 18: 166–175.
19. Ishikawa, J., N. Takahashi, T. Matsumoto, Y. Yoshioka, N. Yamamoto, M. Nishikawa, H. Hibi, N. Ishigro, M. Ueda, K. Furukawa, and A. Yamamoto. 2016. Factors secreted from dental pulp stem cells show multifaceted benefits for treating experimental rheumatoid arthritis. *Bone* 83: 210–219.
20. Wakayama, H., N. Hashimoto, Y. Matsushita, K. Matsubara, N. Yamamoto, Y. Hasegawa, M. Ueda, and A. Yamamoto. 2015. Factors secreted from dental pulp stem cells show multifaceted benefits for treating acute lung injury in mice. *Cytotherapy* 17: 1119–1129.
21. Matsushita, Y., M. Ishigami, K. Matsubara, M. Kondo, H. Wakayama, H. Goto, M. Ueda, and A. Yamamoto. 2015. Multifaceted therapeutic benefits of factors derived from stem cells from human exfoliated deciduous teeth for acute liver failure in rats. *J. Tissue Eng. Regen. Med*. DOI: 10.1002/term.2086.
22. Mita, T., Y. Furukawa-Hibi, H. Takeuchi, H. Hattori, K. Yamada, H. Hibi, M. Ueda, and A. Yamamoto. 2015. Conditioned medium from the stem cells of human dental pulp improves cognitive function in a mouse model of Alzheimer's disease. *Behav. Brain Res.* 293: 189–197.
23. Matsubara, K., Y. Matsushita, K. Sakai, F. Kano, M. Kondo, M. Noda, N. Hashimoto, S. Imagama, N. Ishiguro, A. Suzumura, et al. 2015. Secreted ectodomain of sialic acid-binding Ig-like lectin-9 and monocyte chemoattractant protein-1 promote recovery after rat spinal cord injury by altering macrophage polarity. *J. Neurosci.* 35: 2452–2464.
24. Kato, H., A. Ito, J. Kawanokuchi, S. Jin, T. Mizuno, K. Ojika, R. Ueda, and A. Suzumura. 2004. Pituitary adenylate cyclase-activating polypeptide (PACAP) ameliorates experimental autoimmune encephalomyelitis by suppressing the functions of antigen presenting cells. *Mult. Scler.* 10: 651–659.
25. Wang, J., H. Takeuchi, Y. Sonobe, S. Jin, T. Mizuno, S. Miyakawa, M. Fujiwara, Y. Nakamura, T. Kato, H. Muramatsu, et al. 2008. Inhibition of midkine alleviates experimental autoimmune encephalomyelitis through the expansion of regulatory T cell population. *Proc. Natl. Acad. Sci. USA* 105: 3915–3920.
26. Zhou, Y., Y. Sonobe, T. Akahori, S. Jin, J. Kawanokuchi, M. Noda, Y. Iwakura, T. Mizuno, and A. Suzumura. 2011. IL-9 promotes Th17 cell migration into the central nervous system via CC chemokine ligand-20 produced by astrocytes. *J. Immunol.* 186: 4415–4421.
27. Takeuchi, H., S. Jin, J. Wang, G. Zhang, J. Kawanokuchi, R. Kuno, Y. Sonobe, T. Mizuno, and A. Suzumura. 2006. Tumor necrosis factor-alpha induces neurotoxicity via glutamate release from hemichannels of activated microglia in an autocrine manner. *J. Biol. Chem.* 281: 21362–21368.
28. Takeuchi, H., H. Mizoguchi, Y. Doi, S. Jin, M. Noda, J. Liang, H. Li, Y. Zhou, R. Mori, S. Yasuoka, et al. 2011. Blockade of gap junction hemichannel suppresses disease progression in mouse models of amyotrophic lateral sclerosis and Alzheimer's disease. *PLoS One* 6: e21108.
29. Takeuchi, H., T. Mizuno, G. Zhang, J. Wang, J. Kawanokuchi, R. Kuno, and A. Suzumura. 2005. Neuritic beading induced by activated microglia is an early feature of neuronal dysfunction toward neuronal death by inhibition of mitochondrial respiration and axonal transport. *J. Biol. Chem.* 280: 10444–10454.
30. Jin, S., H. Takeuchi, H. Horiuchi, Y. Wang, J. Kawanokuchi, T. Mizuno, and A. Suzumura. 2014. Fingolimod ameliorates axonal damage in experimental autoimmune encephalomyelitis. *Clin. Exp. Neuroimmunol.* 5: 315–320.
31. Kitamura, K., A. Iwanami, M. Nakamura, J. Yamane, K. Watanabe, Y. Suzuki, D. Miyazawa, S. Shibata, H. Funakoshi, S. Miyatake, et al. 2007. Hepatocyte growth factor promotes endogenous repair and functional recovery after spinal cord injury. *J. Neurosci. Res.* 85: 2332–2342.
32. Deuse, T., C. Peter, P. W. Fedak, T. Doyle, H. Reichenspurner, W. H. Zimmermann, T. Eschenhagen, W. Stein, J. C. Wu, R. C. Robbins, and S. Schrepfer. 2009. Hepatocyte growth factor or vascular endothelial growth factor gene transfer maximizes mesenchymal stem cell-based myocardial salvage after acute myocardial infarction. *Circulation* 120(11, Suppl,)S247–S254.

33. Nakamura, T., K. Sakai, T. Nakamura, and K. Matsumoto. 2011. Hepatocyte growth factor twenty years on: Much more than a growth factor. *J. Gastroenterol. Hepatol.* 26(Suppl, 1): 188–202.
34. Huang, D., Y. Han, M. R. Rani, A. Glabinski, C. Trebst, T. Sørensen, M. Tani, J. Wang, P. Chien, S. O'Bryan, et al. 2000. Chemokines and chemokine receptors in inflammation of the nervous system: manifold roles and exquisite regulation. *Immunol. Rev.* 177: 52–67.
35. Mahad, D. J., and R. M. Ransohoff. 2003. The role of MCP-1 (CCL2) and CCR2 in multiple sclerosis and experimental autoimmune encephalomyelitis (EAE). *Semin. Immunol.* 15: 23–32.
36. McWhorter, F. Y., T. Wang, P. Nguyen, T. Chung, and W. F. Liu. 2013. Modulation of macrophage phenotype by cell shape. *Proc. Natl. Acad. Sci. USA* 110: 17253–17258.
37. Tierney, J. B., M. Kharkrang, and A. C. La Flamme. 2009. Type II-activated macrophages suppress the development of experimental autoimmune encephalomyelitis. *Immunol. Cell Biol.* 87: 235–240.
38. Liu, C., Y. Li, J. Yu, L. Feng, S. Hou, Y. Liu, M. Guo, Y. Xie, J. Meng, H. Zhang, et al. 2013. Targeting the shift from M1 to M2 macrophages in experimental autoimmune encephalomyelitis mice treated with fasudil. *PLoS One* 8: e54841.
39. Meisel, R., A. Zibert, M. Laryea, U. Göbel, W. Däubener, and D. Dilloo. 2004. Human bone marrow stromal cells inhibit allogeneic T-cell responses by indoleamine 2,3-dioxygenase-mediated tryptophan degradation. *Blood* 103: 4619–4621.
40. Djouad, F., L. M. Charbonnier, C. Bouffi, P. Louis-Plence, C. Bony, F. Apparailly, C. Cantos, C. Jorgensen, and D. Noël. 2007. Mesenchymal stem cells inhibit the differentiation of dendritic cells through an interleukin-6-dependent mechanism. *Stem Cells* 25: 2025–2032.
41. Matysiak, M., W. Orlowski, M. Fortak-Michalska, A. Jurewicz, and K. Selmaj. 2011. Immunoregulatory function of bone marrow mesenchymal stem cells in EAE depends on their differentiation state and secretion of PGE2. *J. Neuroimmunol.* 233: 106–111.
42. Bai, L., D. P. Lennon, A. I. Caplan, A. DeChant, J. Hecker, J. Kranso, A. Zaremba, and R. H. Miller. 2012. Hepatocyte growth factor mediates mesenchymal stem cell–induced recovery in multiple sclerosis models. *Nat. Neurosci.* 15: 862–870.
43. Laterza, C., A. Merlini, D. De Feo, F. Ruffini, R. Menon, M. Onorati, E. Fredrickx, L. Muzio, A. Lombardo, G. Comi, et al. 2013. iPSC-derived neural precursors exert a neuroprotective role in immune-mediated demyelination via the secretion of LIF. *Nat. Commun.* 4: 2597.